ELSEVIER

Biophysical Chemistry 77 (1999) 111–121

Biophysical Chemistry

Characterisation by triple-quantum filtered ^{17}O-NMR of water molecules buried in lysozyme and trapped in a lysozyme-inhibitor complex

Evelyne Baguet*, Nicolas Hennebert

Laboratoire d'analyse isotopique et électrochimique de métabolismes, UPRES-A CNRS 6006, Université de Nantes, BP 92208, 2 rue de la Houssinière, F-44322 Nantes cedex 03, France

Received 19 November 1998; received in revised form 1 February 1999; accepted 1 February 1999

Abstract

Triple-quantum filtering NMR sequences were used to study the multiexponential relaxation behaviour of $H_2{}^{17}O$ in the presence of hen egg white lysozyme. By this means, the fraction and the correlation time of water were determined in slow motion, as well as the relaxation time of water in the extreme narrowing limit. The small number of water molecules in slow motion, which is between four and five per lysozyme, seems to correspond to the 'integral' water, buried or in the cleft inside the protein, whereas water in fast motion corresponds to all other water molecules, interacting or not with the macromolecules. The same experiment was performed after addition of the inhibitor tri-*N*-acetylglucosamine $(NAG)_3$. For solutions of sufficient viscosity, there were approximately three supplementary water molecules in slow motion per lysozyme, probably trapped between the protein and the inhibitor. The correlation time of these water molecules was estimated at 2 ns, which should correspond to their residence time in the complex.

Keywords: Lysozyme; Tri-*N*-acetylchitotriose; NMR; ^{17}O-water; Buried water; Quadrupolar relaxation; Triple-quantum filtered spectra

1. Introduction

The water–protein interaction has long been recognised as a major determinant of chain folding, conformational stability, internal dynamics and binding specificity of globular proteins [1]. Until recently, water molecules interacting with proteins have mostly been observed by X-ray diffraction. This powerful technique has shown that crystallised proteins contain a large number of hydration water molecules, mostly at their surface. It has also been observed that a small fraction of water molecules, usually called buried (or internal), occupy internal cavities. Some of these

* Corresponding author. Tel.: +33 2-51125703; fax: +33 2-51125712; e-mail: evelyne.baguet@chimbio.univ-nantes.fr

0301-4622/99/$ - see front matter
PII S0301-4622(99)00015-0

internal water molecules are in the vicinity of interior β-turns that may assume functional roles in their respective proteins [2]. Hence, internal water can be considered as an integral part of the protein molecular architecture. Bound water molecules have also been detected in an antigen–antibody association, which may play a key role in its conformational stabilisation [3].

Unfortunately, X-ray crystallography does not provide a dynamic picture of all these different types of water and, moreover, the behaviour of water in solution may be significantly different from in crystals. In recent years, the study of water/protein systems by various NMR techniques has lead to a better understanding of water relaxation behaviour in the presence of proteins. Nuclear Overhauser enhancement spectroscopy (NOESY) techniques performed on small proteins have been used to demonstrate that only a well-defined, small number of water molecules, which are generally buried, have a long residence time. These are found at identical locations in the crystal structure and in solution, whereas most of the water molecules at the protein surface do not have a well-defined position [4]. Thus, it has been shown that most of the water previously considered as 'heavily-bound' from X-ray measurements is not bound to the proteins in aqueous solution. It is now clear that buried water, despite its small quantity, plays an important role in the global water relaxation behaviour [5–7]. Triple-quantum filtering sequences can also be used to study the multiexponential behaviour of $H_2^{17}O$ in the presence of biological macromolecules and to characterise separately water in slow and in fast motion. A very small fraction of water, found to be in slow motion, has been interpreted as corresponding to strongly-bound water [8–12]. This last method has the advantage over relaxation–dispersion measurements that it does not require experiments to be performed at a wide range of magnetic field strengths. Also, if both transverse and longitudinal relaxations are studied with triple quantum filtered sequences, it allows an independent determination of the contributions to the relaxation of water in slow and fast motion without the need for a preliminary hypothesis about the number of strongly bound water molecules and their average correlation time [8].

The state of hydration of lysozyme, a small globular protein of 14 600 Da, has been studied by a number of techniques which have yielded widely differing values of the amount of strongly bound water. Crystals of the protein contain large amounts of water. Dielectric studies showed that there are approximately 32 water molecules tightly bound, together with four internally bound molecules [13]. X-ray studies gave similar results: there are approximately 140 ordered water molecules per lysozyme, 33–35 of them strongly bound, depending on the origin of the lysozyme. This strongly-bound water fraction contains several water molecules located at the active site and four internally bound molecules located in a semi-circle around the side-chain of Ala92 [14]. Results obtained recently by NMR, however, indicate that the water molecules which are strongly bound in the lysozyme crystal are not necessarily strongly bound in solution: NOE measurements performed by ^{1}H-NMR showed that the residence time of water in the active site of lysozyme is less than 0.5 ns [15]. In fact, only the buried water and a water molecule trapped in a narrow cleft but still accessible to the solvent should have a long residence time in lysozyme [7] and may contribute to a signal after NMR triple-quantum filtered sequence. Lysozyme hydration has already been studied by transverse triple-quantum filtered spectroscopy [10], indicating that approximately one water molecule was strongly bound per lysozyme. However, as the correlation time of strongly bound water was set to 15 ns, which is three times more than the correlation time deduced recently from ^{17}O relaxation analysis at different fields [7], this value may be significantly different from the actual number of water molecules in slow motion.

A crucial facet of protein/water interactions is the role played by water in the formation of the protein–substrate complex. In a crystallographic study of the interactions between lysozyme and an inhibitor, the trisaccharide (NAM-NAG-NAM) [16], Strynadka and James [17] concluded that seven water molecules are displaced from the active-site region by the binding of the trisaccha-

ride. In a similar study of the complexation of lysozyme with $(NAG)_3$, another inhibitor, it was concluded that there were eight ordered water molecules in the active site of lysozyme and that three of these were displaced when $(NAG)_3$ was bound. In view of the widely-differing estimates for bound water obtained by X-ray crystallographic studies and NMR in liquid solutions, it was considered essential to also have a dynamic picture of water trapped in the protein–substrate complex in solution.

This paper reports the simultaneous use of longitudinal and transversal triple-quantum filtering pulse sequences to determine the number of water molecules in slow motion per lysozyme, their correlation time and the relaxation rate of water in fast motion, in the presence or absence of the lysozyme inhibitor $(NAG)_3$. The objective was to determine independently the amount of buried water and to determine the dynamics of the entrapment of water by the inhibitor when binding to lysozyme.

2. Materials and methods

Hen egg white lysozyme, of activity approximately 70 000 U/mg, was obtained from Fluka (L'Isle d'Abeau, France) and *N,N′,N′*-triacetylchitotriose $(NAG)_3$, of purity 95%, from Sigma Aldrich (L'Isle d'Abeau, France). Deuterated water at 99.9% was from Eurisotop (CEA, France) and $H_2\,{}^{18}O$ at 10% (also containing $H_2\,{}^{17}O$ at 0.35%) from CEA-ORIS (France).

2.1. NMR at 9.4 T

Different amounts of lysozyme were diluted in deuterated water with no further preparation. Preliminary measurements showed that this water is slightly enriched in ^{17}O. Samples (3 ml) were studied by ^{17}O-NMR on a Bruker DPX400 spectrometer, in a 10-mm (e.d.) NMR tube, with a broadband probe, at 54.25 MHz. The 90° pulse length was 24 μs. All experiments were performed with an acquisition time set to at least 42 ms, corresponding to 512 points in the time domain, and a supplementary recovery delay of at least 5 ms. No proton decoupling was applied. The acquisition time was significantly larger than 5 T_2 and 5 T_1 but, because of the digital acquisition mode of the spectrometer, no detection was performed during the last 15 ms of the acquisition delay, and a supplementary delay was necessary before the next acquisition pulse. A one-pulse sequence enabled the magnitude of the signal to be estimated. The longitudinal relaxation times were determined with the inversion–recovery pulse sequence. The triple-quantum filtered pulse sequences employed were those described in [18], which are $90° - \tau_e/2 - 180° - \tau_e/2 - 70.5° - \tau_m - 90° - \mathrm{Acq}(t_2)$ and $180° - \tau_e - 70.5° - \tau_m - 90° - \mathrm{Acq}(t_2)$ with appropriate phase cycles, for transverse and longitudinal relaxation, respectively, and with the evolution delay τ_m kept to a minimum at 4 or 5 μs.

2.2. NMR at 11.7 T

Hen egg white lysozyme was diluted in a mixture of 80% $H_2^{18}O$ at 10 and 20% of D_2O at 99.9% with no further preparation. Probably because of its method of preparation, water enriched in ^{18}O is also enriched in ^{17}O. Hence, this mixture corresponded to water enriched in ^{17}O approximately five times more than in deuterated water. Two samples were prepared, of lysozyme concentrations 15% w/v and 20% w/v. They were studied before and after addition of tri *N*-acetylglucosamine $(NAG)_3$, a lysozyme inhibitor added in excess (1.5 times and twice the concentration of lysozyme for the two samples, respectively). The binding rate constant of $(NAG)_3$ to lysozyme is $1.3 \times 10^2\ s^{-1}$ at 45°C [19], and its binding constant is $1 \times 10^5\ M^{-1}$ [20]. Thus, for the concentrations employed, almost all the lysozyme was complexed with $(NAG)_3$ and this complex was stable enough to be studied on its own by NMR. Samples (0.6 ml) were studied by ^{17}O-NMR on a Bruker DRX500 spectrometer, in a 5-mm (e.d.) NMR tube, with a inverse-detection broadband probe, at 67.80 MHz. The 90° pulse length was 14 μs. T_2 measurements were performed with the Hahn-echo pulse sequence. Other parameters were the same as at 9.4 T.

2.3. Processing

The signals detected after the triple quantum filtered pulse sequences are called $s^{(1)}(\tau_e)s^{(1)}(t_2)$ and $s^{(0)}(\tau_e)s^{(1)}(t_2)$ for transverse and longitudinal magnetisation, respectively. The function $s^{(1)}(t)$ was deduced from the 'transverse' triple-quantum-filtered signal detected in the time domain for a given value of τ_e. The corresponding FID was transformed in an ASCII file and studied on a power Macintosh. The function $s^{(0)}(t)$ was studied by comparing the amplitude of the 'longitudinal' and 'transverse' triple-quantum-filtered signals after Fourier transformation. For this, the FIDs from the triple-quantum-filtered signals were zero filled to 512 points and an exponential line-broadening of 20 Hz was applied prior to Fourier transformation.

2.4. Analysis

The functions $s^{(0)}(t)$ and $s^{(1)}(t)$ are characteristic of the relaxation behaviour and can be related to the fraction of water in slow motion, p_s, its correlation time, τ_s, and the relaxation rate, R_{bulk}, of water in fast motion, which corresponds in our case to free water and water weakly bound to the protein [8,18]. Because ^{17}O has a spin of 5/2, both transverse and longitudinal magnetisation's of ^{17}O-water in slow motion evolve triexponentially [21]. Their relaxation behaviours are described by 3×3 relaxation matrices $\mathbf{R}_s^{(1)}$ and $\mathbf{R}_s^{(0)}$, respectively, whose components depend on the product $\omega_0\tau_c$ and on the quadrupolar constant $(e^2qQ/h)(1+\eta^2/3)^{1/2}$ of ^{17}O-water in slow motion [18]. The magnetisation of bulk water alone would evolve monoexponentially with the rate constant R_{bulk}. In the same basis set as that employed for water in slow motion, it has a diagonal relaxation matrix $\mathbf{R}_{\text{bulk}}$ which depends only on the value of R_{bulk}. The global relaxation matrices of water are then: $\mathbf{R}_{\text{water}}^{(n)} = p_s\mathbf{R}_s^{(n)} + (1-p_s)\mathbf{R}_{\text{bulk}}$, where n is equal to 0 or 1 for longitudinal or transverse magnetisation, respectively. The functions $s^{(0)}(t)$ and $s^{(1)}(t)$ were calculated by diagonalisation of water relaxation matrix. For this, the value of the quadrupolar constant $(e^2qQ/h)(1+\eta^2/3)^{1/2}$ was taken to be the same as for D_2O ice: 6.5 MHz, following previous work performed by Denisov et al. [6]. For given values of p_s and τ_s (the fraction and correlation time of water in slow motion), R_{bulk} was deduced from the longitudinal relaxation rate constant of water [8]. The relaxation matrices $\mathbf{R}_{\text{water}}^{(n)}$ were then calculated and diagonalised. Water magnetisation time-course after triple-quantum-filtered experiments was calculated, with its amplitude deduced from the intensity of the water signal after a one-pulse measurement [8]. The parameters p_s and τ_s were then adjusted for an optimal correspondence between theory and experiment. This enabled the determination of the fraction of water in slow motion, its correlation time, and the relaxation rate R_{bulk} of water in fast motion. Simultaneously, the accuracy of these values could be estimated.

3. Results and discussion

3.1. Unique nature of the solution

Firstly, it is important to confirm that a single pair of values p_s and τ_s does fit the experimental data of a given sample. It has been shown that these two parameters could not be deduced independently from the decay of the transverse triple-quantum filtered (TQF) signal of ^{17}O-water alone [10]. However, in the present case, longitudinal TQF signal was also studied. So as to show that these two experiments are sufficient for determining p_s and τ_s, simulations of the signals detected after triple-quantum filters have been performed. All numerical values, except the unknowns R_{bulk}, p_s and τ_s, were the same as for a typical experiment. Then, the matrices of water in slow motion were functions of p_s and τ_s. The apparent longitudinal relaxation rate of water interacting with proteins, which corresponds with a good approximation to $R_1^{(0)}$, was set to 260 s^{-1}, a value in the range found experimentally for various samples. It was assumed that both longitudinal and transversal TQF signals evolved biexponentially. The validity of this approximation has already been checked for longitudinal relaxation [8]. From this approximation, it is possible to define R_{bulk} as a function of p_s and τ_s, and then

to determine analytically the signal detected after the longitudinal triple-quantum filter. This approximation is less good for transverse magnetisation, whose relaxation is more multiexponential. Then, it involves a small systematic error on the numerical value of the signal after the triple-quantum filter, but without modifying its behaviour significantly. Also, it allows an analytical value of the transverse TQF signal as a function of p_s and τ_s, for a given value of the delay τ_e, to be obtained.

The signal detected after a longitudinal or transverse triple-quantum filter reaches a maximum for:

$$t_{\max}^{(n)} = \frac{\ln(R_{\mathrm{I}}^{(n)}) - \ln(R_{\mathrm{III}}^{(n)})}{R_{\mathrm{I}}^{(n)} - R_{\mathrm{III}}^{(n)}} \quad (1)$$

where $n = 0$ or 1 depending on the experiment performed.

The maximal amplitude in the time domain of the signal detected after a transverse TQF experiment is then obtained at $t_{\max}^{(1)}$ and for $\tau_e = t_{\max}^{(1)}$. Its simulation is represented in Fig. 1 for various values of p_s and τ_s. It can seen that the signal increases with both p_s and τ_s in the range studied (p_s between 10^{-4} and 10^{-2} and τ_s between 1.5 and 20 ns). The signal detected after a longitudinal TQF sequence was simulated in a similar way, for $\tau_e = t_{\max}^{(0)}$. The signal represented in Fig. 2 corresponds to the amplitude of the longitudinal TQF signal obtained after Fourier transformation, compared to the corresponding transverse TQF signal for the same τ_e and for which the amplitude after Fourier transformation was set to a constant value. It can seen that, for $\tau_s > 4$ ns, this signal increases with p_s and decreases with τ_s whatever the values of p_s in the range studied. In this case, for given values of the signals after triple-quantum filters, there is a unique pair of solutions p_s and τ_s. However, no direct conclusion can be given for smaller values of τ_s. So as to verify that there is a unique solution in all cases, the contour plots of the two curves are drawn in Fig. 3. Clearly, for the simulation of each experiment, after a transverse (dots) or longitudinal (straight line) triple-quantum filter, a given amplitude corresponds to many different pairs of values p_s and τ_s. This confirms the results already obtained in [10]. Nevertheless, two curves corresponding to signals after longitudinal and transverse triple-quantum filters are seen not to cross

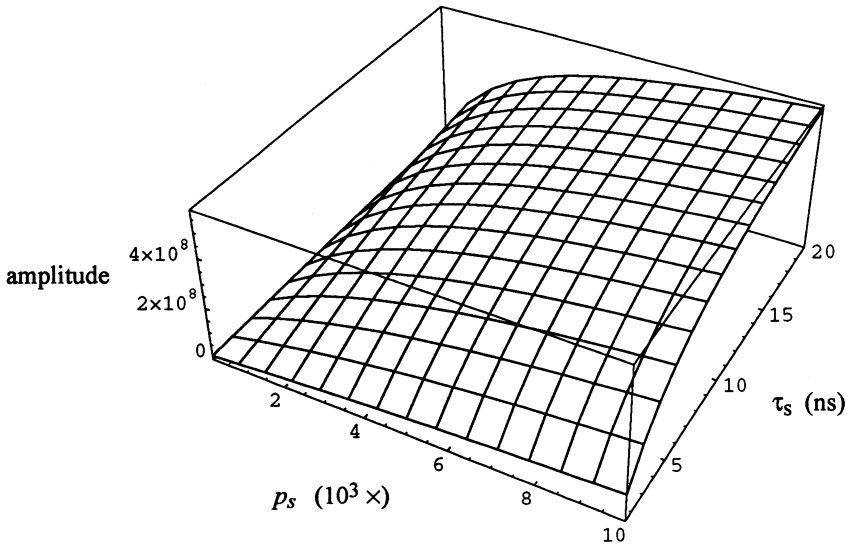

Fig. 1. Simulation of the maximal amplitude of the signal detected in the time domain after a transverse triple-quantum filtered NMR sequence as a function of p_s, the fraction of water in slow motion and τ_s, its correlation time. The amplitude was calibrated from the signal detected after a one-pulse sequence.

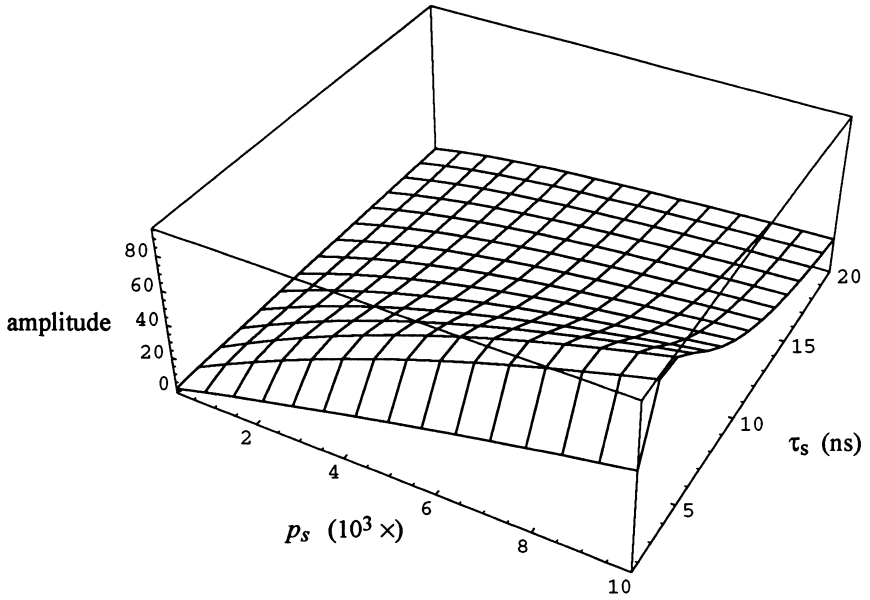

Fig. 2. Simulation of the maximal amplitude of the signal detected in the frequency domain after a longitudinal triple-quantum filtered NMR sequence as a function of p_s, the fraction of water in slow motion and τ_s, its correlation time. The amplitude is calibrated to that obtained after a transverse triple-quantum filtered sequence and set to a constant value.

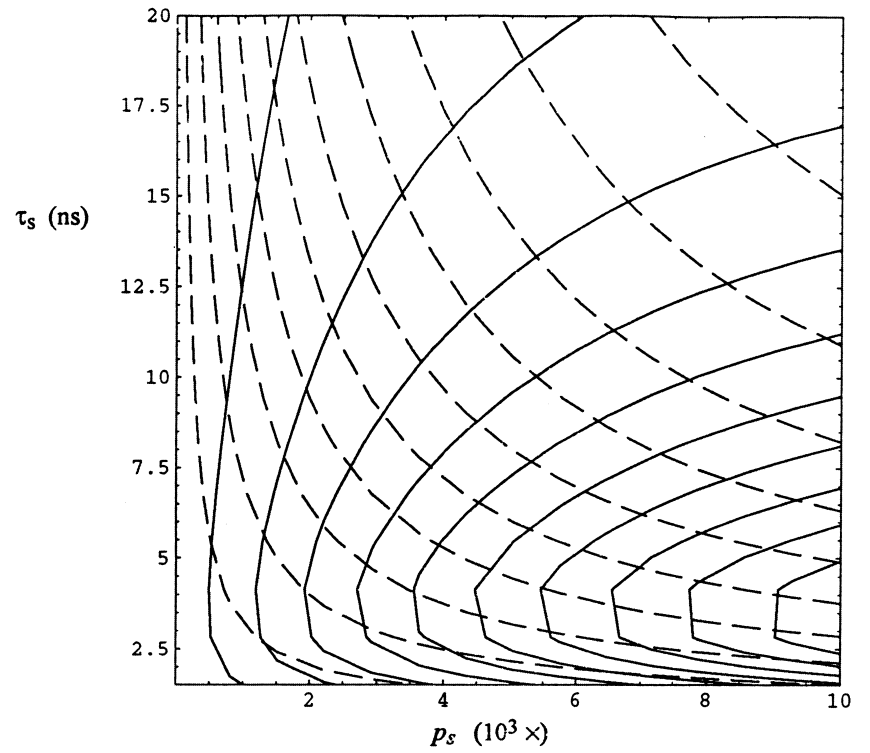

Fig. 3. Contour plot of the curves drawn in Fig. 1 (transverse TQF signal - - -) and in Fig. 2 (longitudinal TQF signal —).

each other more than once, meaning that, for a given pair of amplitudes, there is no more than one pair of p_s and τ_s which corresponds to the exact solution.

These simulations have been repeated for various values of $R_1^{(0)}$ between 230 and 385 s^{-1}, the extreme limits found for the different samples studied. Similar curves to the one of Fig. 3 were found in all cases. From these simulations, it can be concluded that a unique pair of values p_s and τ_s does fit the data of the different samples studied in this work.

3.2. Detection of water in slow motion

Aqueous solutions of lysozyme at different concentrations were analysed at 28°C. The number of water molecules in slow motion per lysozyme molecule was calculated for the different concentrations. The results are given in Table 1. The relaxation rate of water in fast motion R_{bulk} and the correlation time τ_s of water in slow motion both increase at higher lysozyme concentrations. The number of water molecules in slow motion per lysozyme does not change significantly with the concentration, except at 10% w/v where no water in slow motion was detected, presumably due to its correlation time being too short. This water in slow motion should correspond to the buried and cleft water detected previously by other methods. It has a correlation time between 4 and 6 ns, which is of the same order as that found by ^{17}O relaxation analysis at different field strengths (5.3 ns) [7] and close to the correlation time deduced from the Debye–Stoke–Einstein relationship (4.2 ns) [22]. The small number of water molecules in slow motion, approximately 4, is close to those found by ^{17}O magnetic relaxation measurements at different fields [7,23] but significantly higher than that obtained by transverse triple-quantum filtered relaxation analysis [10]. In these later experiments, however, the quadrupolar constant of water in slow motion was set to 7.6 MHz, which is adequate for free and weakly bound water, but not for internal water, and the correlation time of this water was kept to 15 ns, which is almost three times more than the correlation time deduced recently from ^{17}O relaxation analysis at different field strengths (5.3 ns) [7]. In fact, it is particularly important to know the correlation-time value of water in slow motion is for the water signal analysis. If this was set to 15 ns and analysed in the same way as in Torres et al. [10], not only would the number of water molecules in slow motion deduced from the transverse triple-quantum filtered experiment be changed, but also the value of R_{bulk}. Then, the fraction of weakly bound water deduced from R_{bulk} would be overestimated by approximately 30%. In the present case, the intensity of the signal measured after longitudinal triple-quantum filtered experiments allows the unambiguous conclusion that the correlation time of water in slow motion is not 15 ns: if the correlation time of water were to be equal to 15 ns, the intensity of this signal would be seven times larger than measured. Thus, from the experimental data presented here, it can be deduced unambiguously that, at 28°C and for sufficiently high concentrations of lysozyme, there are approximately four water molecules in slow motion. Depending on the concentration, their correlation times are between 4 and 6 ns.

The validity of the results depends on the model employed, which supposes that there is fast exchange between two populations. This model could give inadequate results if the different water molecules in slow motion were to have different correlation times. Then, a model with a distribution of correlation times should be employed [24]. However, in the present case, there

Table 1
Water 'properties' for lysozyme aqueous solutions at 28°C

Lysozyme concentration (w/v)	R_{bulk} (s^{-1})	p_s ($10^3\times$)	τ_s (ns)	$n_{s/Lyso}$
0	174 ± 1	0	–	–
15	211 ± 2	0.89 ± 0.05	4.1 ± 0.3	4.4 ± 0.4
20	226 ± 2	0.95 ± 0.05	5.1 ± 0.3	3.8 ± 0.4
30	258 ± 2	1.6 ± 0.1	5.2 ± 0.3	4.3 ± 0.3
40	301 ± 2	2.2 ± 0.1	6.1 ± 0.3	4.3 ± 0.2

R_{bulk}, relaxation rate constant of bulk (free + weakly bound) water; p_s, fraction of water in slow motion; τ_s, correlation time of water in slow motion; $n_{s/Lyso}$, number of water molecules in slow motion per lysozyme molecule.

are very few water molecules in slow motion per protein and, even if their correlation times were not exactly the same, they should not be very different. Hence, the model employed should give a good picture of the mobility of water in slow motion, though it must be borne in mind that the mean correlation time deduced from the model may differ slightly from the correlation times for each water molecule in slow motion.

The solutions of lysozyme were studied in the same way at 25°C, so as to determine whether at a lower temperature some water molecules in slow motion could be detected, even at very low concentrations. Approximately five water molecules in slow motion were detected, even at 10% w/v concentration (Table 2). Thus, it seems that the detection of water in slow motion is not perturbed by any aggregation behaviour of the protein. From these results it can be deduced that not all the water in slow motion has the same correlation time when the temperature increases. Approximately one water molecule (probably cleft water) would appear to have a smaller correlation time. This molecule would be in slow motion at 25°C but at higher temperatures, as the viscosity decreases, it would have a correlation time small enough for its magnetisation to be in the extreme narrowing limit, whereas the other four molecules would still be in the slow motion limit. This being so, the correlation time of water in slow motion at lower temperatures would be slightly smaller than that of the protein and would also depend on the water residence time in the protein. Hence, this experimental approach performed very precisely and analysed via an adequate model of the different types of water in slow motion could be used to determine the residence time in the protein of the most mobile of 'integral' water. Such results could be obtained, however, only with much more precise experiments, probably necessitating the use of highly enriched water.

Two solutions of lysozyme (30% w/v or 40% w/v) were also studied at various temperatures (Fig. 4). In both cases, the number of water molecules in slow motion decreased with temperature, from five at 25°C to less than four at 37°C, whereas their correlation times — approximately 5 ns for lysozyme 30% w/v and 6 ns for lysozyme 40% w/v — did not change significantly. On the other hand, at a given temperature, the number of water molecules in slow motion per lysozyme was not very different for concentrations of 30% w/v or 40% w/v. These results can be interpreted in a similar way as for the solutions studied at 25 and 28°C. They also show that the results obtained are reproducible.

Table 2
Water 'properties' for lysozyme aqueous solutions at 25°C

Lysozyme concentration (w/v)	R_{bulk} (s^{-1})	p_s ($10^3 \times$)	τ_s (ns)	$n_{s/Lyso}$
10	211 ± 2	0.65 ± 0.05	3.2 ± 0.3	5.0 ± 0.4
15	232 ± 2	1.04 ± 0.08	3.7 ± 0.3	5.0 ± 0.4
20	241 ± 2	1.3 ± 0.1	4.8 ± 0.3	5.4 ± 0.4
30	294 ± 2	1.9 ± 0.1	5.2 ± 0.3	5.1 ± 0.3
40	339 ± 2	2.4 ± 0.1	6.6 ± 0.3	4.8 ± 0.2

R_{bulk}, relaxation rate constant of bulk water; p_s, fraction of water in slow motion; τ_s, correlation time of water in slow motion; $n_{s/Lyso}$, number of water molecules in slow motion per lysozyme molecule.

3.3. Interaction of lysozyme with an inhibitor

Different solutions of lysozyme were studied in a 11.7-T spectrometer, before and after the addition of the lysozyme inhibitor $(NAG)_3$. The principal ^{17}O-water relaxation data measured are given in Table 3. For each sample, the addition of $(NAG)_3$ leads to a decrease of T_1 and T_2, a very weak increase of the signal detected after a transverse triple-quantum filter and a more significant increase of the signal detected after the longitudinal triple-quantum filter sequence.

These samples were analysed in the same way as those studied at 9.4 T. The results obtained are summarised in Table 4. For samples without the addition of $(NAG)_3$, the number of water molecules in slow motion per lysozyme was the same as at 9.4 T at a similar temperature. For ease of interpretation, we will consider that this corresponds to the 'integral' water. For lysozyme 15% w/v at 25°C and lysozyme 20% w/v at 30°C, R_{bulk} did not change significantly after the addition of $(NAG)_3$, whereas there were approximately three more water molecules in slow mo-

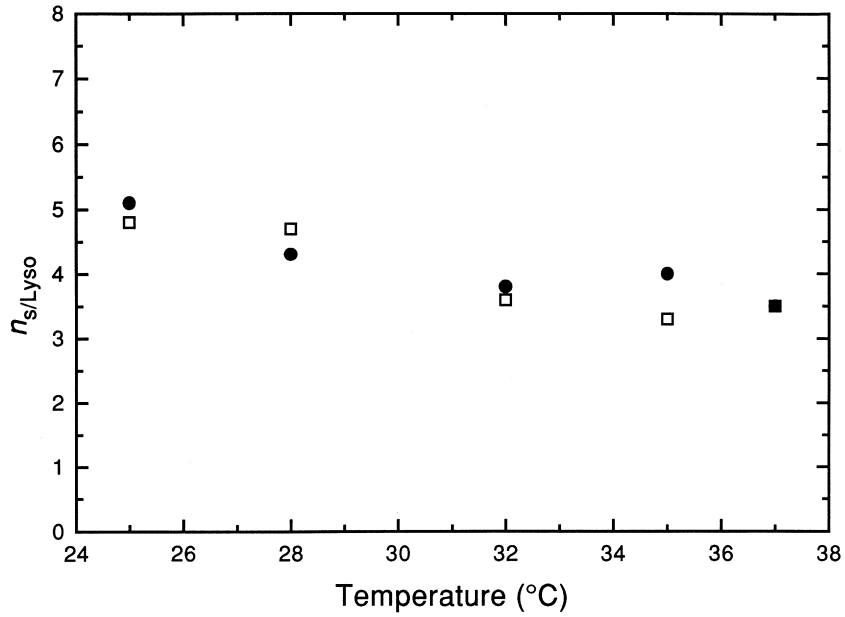

Fig. 4. Number of water molecules in slow motion per lysozyme as a function of the temperature. Two different concentrations were studied, lysozyme 30% w/v in D_2O (●) and lysozyme 40% w/v in D_2O (□).

tion and their correlation time was diminished (Table 4). In contrast, when lysozyme 15% w/v was studied at 30°C, no significant changes were observed after addition of $(NAG)_3$, probably because the correlation time of the trapped water was too small to be characterised precisely by this method.

From these results, it can be concluded that, when the sample is of sufficient viscosity, approximately three supplementary water molecules in

Table 3
Effect of $(NAG)_3$ addition upon ^{17}O-water relaxation data for lysozyme aqueous solutions

Temperature	Sample	T_1 (ms)	T_2 (ms)	$s^{(1)}$ (1.8 ms)	$s^{(0)}$ (2.6 ms)
25°C	15% w/v	4.70 ± 0.01	3.74 ± 0.01	91 ± 1	64 ± 1
	15% w/v + $(NAG)_3$	4.46 ± 0.01	3.46 ± 0.01	100 ± 1	77 ± 1
30°C	15% w/v	5.39 ± 0.01	4.31 ± 0.01	91 ± 1	70 ± 1
	15% w/v + $(NAG)_3$	5.13 ± 0.01	3.99 ± 0.01	100 ± 1	88 ± 1
30°C	20% w/v	4.85 ± 0.01	3.55 ± 0.01	93 ± 1	58 ± 1
	20% w/v + $(NAG)_3$	4.46 ± 0.01	3.17 ± 0.01	100 ± 1	73 ± 1

T_1 and T_2 are the apparent longitudinal and transverse relaxation times of water obtained from inversion–recovery and Hahn-echo sequences, respectively. $s^{(1)}$ and $s^{(0)}$ are the relative amplitudes of the transverse and longitudinal signal after a triple quantum filter for a given value of τ_e. For each sample, $s^{(0)}(\tau_e)$ was compared to $s^{(1)}$ (1.8 ms) set to 100. For a given sample $s^{(1)}$ (1.8 ms) was at the same scale with and without addition of $(NAG)_3$.

Table 4
Effect of $(NAG)_3$ addition upon water 'properties' of lysozyme aqueous solutions

Temperature	Sample	R_{bulk} (s^{-1})	p_s ($10^3 \times$)	τ_s (ns)	$n_{s/Lyso}$
25°C	15% w/v	195 ± 2	0.93 ± 0.07	3.6 ± 0.3	5.0 ± 0.4
	15% w/v + $(NAG)_3$	195 ± 2	1.4 ± 0.07 (0.55 ± 0.03)	3.2 ± 0.3 (2.1 ± 0.2)	7.5 ± 0.4 (2.9 ± 0.4)
30°C	20% w/v	187 ± 2	1.1 ± 0.1	4.3 ± 0.3	4.4 ± 0.4
	20% w/v + $(NAG)_3$	186 ± 2	1.9 ± 0.1 (0.90 ± 0.05)	3.4 ± 0.3 (1.9 ± 0.2)	7.5 ± 0.4 (3.6 ± 0.4)

R_{bulk}, relaxation rate constant of bulk water; p_s, fraction of water in slow motion; τ_s, correlation time of water in slow motion; $n_{s/Lyso}$, number of water molecules in slow motion per lysozyme molecule. The specific properties of the water trapped by $(NAG)_3$ when binding to lysozyme, calculated from a model, are given in brackets.

slow motion are detected, which could be trapped when $(NAG)_3$ binds to lysozyme. When the viscosity is too low, however, the correlation time of these molecules is too short for them to give a significant signal after the triple-quantum filter.

The correlation time found after the addition of $(NAG)_3$ is an average for that of water buried or in the cleft of lysozyme in the absence of $(NAG)_3$ and water trapped by the inhibitor. The fact that it is less than the correlation time of the 'integral' water detected without $(NAG)_3$ suggests that the correlation time of trapped water is significantly shorter than that of 'integral' water. In order to obtain a more precise picture of water behaviour in the presence of the inhibitor, simulations were performed of the water-magnetisation time course for three different populations in fast chemical exchange: 'integral' water, for which the correlation time and fraction were set the same as without $(NAG)_3$, trapped water, also in slow motion, and water in the extreme narrowing limit. The fraction and correlation time of trapped water were then adjusted to fit the experimental data. With this model, there were approximately three water molecules trapped by the inhibitor and with a correlation time of 2 ns, which should correspond to their residence time (Table 4).

These results were compared with the coordinates in the Brookhaven protein data bank (PDB) [25] of lysozyme in co-crystal with ligand $(NAG)_3$, (PDB accession code 1HEW [17]). The eight water molecules in the active site of lysozyme should not be heavily bound in solution. On the other hand, when $(NAG)_3$ binds to lysozyme, the three water molecules in site C: OW0 142, OW7 141, OW8 141 (also numbered 74, 75 and 76) should be trapped. The two other water molecules bound in the crystal, OW0 140 and OW5 139, should exchange more easily with the bulk water. The three water molecules OW0 142, OW7 141, OW8 141 may correspond to the supplementary water molecules in slow motion detected by ^{17}O-NMR after addition of the inhibitor.

4. Conclusion

The simultaneous analysis of data from transverse and longitudinal triple-quantum filtered NMR experiments enables the number of water molecules in slow motion, together with their average correlation time, to be determined. The number of such water molecules found corresponds with a good approximation to the 'integral' water in lysozyme, which has a longer residence time than the surface water. Globally, the results found are very close to those obtained by nuclear magnetic relaxation dispersion, but without the need to work at different field strengths. Additionally, it has been shown that three water molecules are trapped when the inhibitor $(NAG)_3$ binds to lysozyme and that these have a residence time of approximately 2 ns, significantly shorter than that of the 'integral water' molecules. To our knowledge, such a fine characterisation has never been performed previously. The method employed here should be use-

ful for characterising the properties of buried or trapped water both in proteins and in protein–ligand complexes. It should also be useful for the study of the water of long residence time in DNA. Contrary to the study of macromolecule hydration by ^{1}H-cross-relaxation, this method is not limited by the size of the macromolecule, as it is only the water that is studied.

Acknowledgements

Julien Thébaud is acknowledged for his help with curve fitting and simulations. Michel Trierweiler and Françoise Mabon are thanked for assistance with the NMR spectrometer; Prof. Charles Tellier for enlightening discussions, advice and for proposing the experiments with inhibitors; and Dr Richard Robins for carefully reading of the manuscript. The regional and departmental administrations of 'Pays de la Loire' are also thanked for the financial assistance with purchasing the inverse gradient probe.

References

[1] F.C. Colombo, D.C. Rau, V.A. Parsegian, Science 256 (1992) 655.
[2] G.D. Rose, W.B. Young, L.M. Gierasch, Nature 304 (1983) 654.
[3] N.T. Bhat, G.A. Bentley, G. Boulot, et al., Proc. Natl. Acad. Sci. U.S.A. 91 (1994) 1089.
[4] G. Otting, E. Liepinsh, K. Wüthrich, Science 254 (1991) 974.
[5] V.P. Denisov, B. Halle, J. Mol. Biol. 245 (1995) 298.
[6] V.P. Denisov, B. Halle, J. Mol. Biol. 245 (1995) 682.
[7] V.P. Denisov, B. Halle, Faraday Discuss. 103 (1996) 227.
[8] E. Baguet, B.E. Chapman, A.M. Torres, P.W. Kuchel, J. Magn. Reson. series B 111 (1996) 1.
[9] E. Baguet, N. Hennebert, B.E. Chapman, A.M. Torres, P.W. Kuchel, J. Magn. Reson. Chem. 35 (1997) S47–S51.
[10] A.M. Torres, S.M. Grieve, B.E. Chapman, P.W. Kuchel, Biophys. Chem. 67 (1997) 187.
[11] A.M. Torres, S.M. Grieve, P.W. Kuchel, Biophys. Chem. 70 (1998) 231.
[12] S.M. Grieve, B. Wickstead, A.M. Torres, P. Styles, S. Wimperis, P.W. Kuchel, Biophys. Chem. 73 (1998) 137.
[13] S. Bone, R. Pethig, J. Mol. Biol. 181 (1985) 323.
[14] C.C.F. Blake, W.C.A. Oulford, P.J. Artymiuk, J. Mol. Biol. 167 (1983) 693.
[15] G. Otting, E. Liepinsh, B. Halle, U. Frey, Nat. Struct. Biol. 4 (1997) 396.
[16] N.C.J. Strynadka, M.N.G. James, J. Mol. Biol. 220 (1991) 401.
[17] J.C. Cheetham, P.J. Artymiuk, D.C. Phillips, J. Mol. Biol. 224 (1992) 613–628.
[18] C.-W. Chung, S. Wimperis, Mol. Phys. 76 (1992) 47.
[19] C.M. Dobson, The structure of lysozyme in solution, in: R.A. Dwek, I.D. Campbell, R.E. Richards, R.J.P. Williams (Eds.), NMR in Biology, Academic Press, London, 1977, p. 63.
[20] S. Kuramitsu, K. Ikeda, K. Hamaguchi, S. Miwa, T. Nishina, J. Biochem. 72 (1972) 1109.
[21] A. Abragam, Les Principes du Magnétisme Nucléaire, Presses Universitaires de France, Paris, France, 1961.
[22] B. Halle, T. Andersson, S. Forsén, B. Lindman, J. Am. Chem. Soc. 103 (1981) 500.
[23] S.H. Koenig, K. Hallenga, M. Shporer, Proc. Natl. Acad. Sci. U.S.A. 72 (1975) 2667.
[24] W.D. Rooney, C.S. Springer, Jr., NMR Biomed. 4 (1991) 209.
[25] F.C. Bernstein, T.F. Koetzle, G.J.B. Williams, et al., J. Mol. Biol. 112 (1977) 535.